JABFM
eISSN 2280-8000

J Appl Biomater Funct Mater 2016; 00(00): 000-000
DOI: 10.5301/jabfm.5000325

ORIGINAL RESEARCH ARTICLE

Open Access

Effect of graphene oxide on bacteria and peripheral blood mononuclear cells

Jessica Campos-Delgado[1], Kelly L.S. Castro[2], Jose G. Munguia-Lopez[3], Ana K. González[1], Martin E. Mendoza[2], Benjamin Fragneaud[4], Raphael Verdan[2], Joyce R. Araujo[2], Francisco J. González[1], Hugo Navarro-Contreras[1], Ivan N. Pérez-Maldonado[1], Antonio de León-Rodríguez[3], Carlos A. Achete[2]

[1] CIACYT, Universidad Autónoma de San Luis Potosí, San Luis Potosí - México
[2] DIMAT, INMETRO, Xerem, Rio de Janeiro - Brazil
[3] Department of Molecular Biology, IPICYT, San Luis Potosí - México
[4] Departamento de Física, UFJF, Juiz de Fora - Brazil

ABSTRACT

Background: Driven by the potential biological applications of graphene, many groups have studied the response of cells exposed to graphene oxide (GO). In particular, investigations of bacteria indicate that there are 2 crucial parameters, which so far have only been investigated separately: GO size and exposure methodology. Our study took into account both parameters. We carefully characterized the samples to catalog sizes and structural properties, and tested different exposure methodologies: exposure in saline solution and in the presence of growth media. Furthermore, we performed experiments with peripheral blood mononuclear cells exposed to our GO materials.

Methods: Atomic force microscopy, scanning electron microscopy, Raman spectroscopy, X-ray photoelectron spectroscopy and transmission electron microscopy were used to characterize the morphology and composition of different samples of GO: GO-H_2O, GO-PBS and GO-MG. Our samples had 2D sizes of ~100 nm (GO-H_2O and GO-PBS) and >2 μm (GO-MG). We tested antibacterial activity and cytotoxicity toward peripheral blood mononuclear cells of 3 different GO samples.

Results: A size-dependent growth inhibition of *Escherichia coli* (DH5 α) in suspension was found, which proved that this effect depends strongly on the protocol followed for exposure. Hemocompatibility was confirmed by exposing peripheral blood mononuclear cells to materials for 24 hours; viability and apoptosis tests were also carried out.

Conclusions: Our experiments provide vital information for future applications of GO in suspension. If its antibacterial properties are to be potentiated, care should be taken to select 2D sizes in the micrometer range, and exposure should not be carried out in the presence of grow media.

Keywords: Antibacterial effect, *Escherichia coli*, Graphene oxide, Peripheral blood mononuclear cells

Introduction

The attention that graphene has attracted since its isolation in 2004 is undeniable (1). Over the years, an increasing number of scientific groups have been seduced by its amazing electronic, mechanical, optical and thermal properties, and evidently, by its innumerable potential applications (2). However, due to the hydrophobic nature of pristine graphene, in biomedicine, graphene oxide (GO) is considered a better alternative thanks to its hydrophilicity, amphiphilicity and availability of functional groups attached to its surface or edges (3). Along with the debut of graphene and GO in biological applications has come the necessity of studying their biocompatibility (4-13). Of particular interest have been the reported antibacterial properties of GO (5, 7-11, 14). Akhavan and Ghaderi (7) argued that the adverse effect of graphene on bacteria is to be attributed to membrane damage by the numerous sharp edges of GO, while others have focused on oxidative stress as the toxic mechanism (8). A recent paper by Mangadlao and coauthors (15) reported on the fabrication of GO films through the Langmuir-Blodgett technique, where graphene sheets lie flat on a polyethylene terephthalate (PET) substrate. Thus the sharp edges of GO were not available to pierce the membranes, and yet antibacterial activity was still observed, suggesting that the antibacterial activity of GO does not rely on membrane damage by its sharp edges. Liu and coauthors (14) conducted experiments that showed that

Accepted: July 4, 2016
Published online: September 7, 2016

Corresponding author:
Dr. Jessica Campos-Delgado
Arquitectos 135
Col. Himno Nacional
CP 78280
San Luis Potosí, SLP, México
jessica.mex@gmail.com

the antibacterial effect of GO depends on the sheet size, suggesting that large graphene sheets wrap bacteria and block interactions, isolating them from the environment, while small sheets interact with bacterial surfaces in a nonharmful way. These results confirmed the encapsulation by graphene reported previously by another group in 2011 (16). Many groups have studied the response of bacteria exposed to GO, and although many researchers have agreed on its antibacterial effect (5, 7, 8, 11, 13), a couple of research groups have reported a contrary effect (9, 10). Ruiz et al (9) confirmed a GO enhancement effect on *Escherichia coli* proliferation, and Das et al (10) confirmed the kinetic growth of *Pseudomonas aeruginosa* and *E. coli* in the presence of GO. These early controversial reports have led to more investigations into the subject. Recently, Hui and coworkers (17) conducted experiments where they demonstrated that the discrepancies regarding the antibacterial effects of GO lie in the way that GO is exposed to the bacteria. When bacteria is exposed to GO in pure saline solution, the antibacterial effect is observed; however, this antibacterial activity decreases progressively when increasing amounts of Luria-Bertani (LB) broth are added to the saline solution. They attribute this decrease of bactericidal activity to the absorption of LB molecules on the surface of the graphene; hence, the more the graphene surface is free from adsorbates, the greater the antibacterial effect it will have. Although this piece of research is very valuable and clarifies the controversial results above discussed, it lacks important information about the characterization of the GO used and does not take into account the size-dependent antibacterial effect reported by Liu and coauthors (14). Moreover, an inspection of the GO materials shown on their figures demonstrates a size-heterogeneous sample.

As described above, different groups have attempted to study the antibacterial effect of graphene and have found 2 major influential parameters: size and exposure methodology. Our study brought together both approaches. We carefully characterized the samples to catalog the sizes and structural properties and tested different exposure methodologies: exposure in saline solution and exposure in the presence of growth media. Our results indicated that the antibacterial effect was not only size dependent but also depended on the exposure technique.

When it comes to cytotoxicity toward mammalian cells, the picture is not any more uniform (4, 12, 13, 18-25). Some groups have reported on the biocompatibility of graphene (4, 13, 18, 21-23, 25), while others have discussed its toxicity in terms of concentration and degree of oxidation (12, 19, 20, 26). The same dilemma applies to its hemocompatibility (12, 22, 27, 28). In any case, many authors who have written reviews on this topic (23-25, 29, 30) have agreed on the need to standardize protocols for the evaluation of cytotoxicity, because many studies are not comparable due to differences in synthesis and processing methods of GO which yield a wide spectrum of physicochemical properties. Sheet size, surface functionalization, degree of oxidation, purity and defects are some of the parameters of GO that vary from one report to the other, rendering it very difficult to draw conclusions from the available literature.

We carried out atomic force microscopy (AFM), scanning and transmission electron microscopy (SEM and TEM), Raman spectroscopy and X-ray photoelectron spectroscopy (XPS) to study the morphology and structure of different GO materials. We also performed an exhaustive series of experiments to test the effects of our GO samples on bacteria and mammalian cells. We produced graphite oxide (GtO) from expanded graphite using the modified Hummers' method, followed by a purification process (see "Materials and methods" and "Supplementary material", available online at www.jab-fm.com). Using this GtO, we obtained 3 different materials: GO dispersed in water for 6 hours in an ultrasonic bath (GO-H_2O), GO dispersed in phosphate-buffered saline (PBS) for 6 hours in an ultrasonic bath (GO-PBS) and GO manually ground and dispersed in water (GO-MG). We confirmed that the antibacterial effect of GO is size dependent and proved that the protocol for exposure plays a crucial role. Our experiments with peripheral blood mononuclear cells (PBMCs) confirmed the hemocompatibility of our different GO materials for the exposure protocol used.

Materials and Methods

GO preparation

We obtained graphite oxide from expanded graphite (from Nacional de Grafite, Brasil) using the modified Hummers' method, followed by a purification process. We dispersed graphite oxide in H_2O or PBS by sonication (ultrasonic bath) for 6 hours, thus obtaining GO-H_2O and GO-PBS, respectively. The sample GO-MG was obtained by manually grinding graphite oxide using a mortar (for further details, see "Supplementary material").

Raman spectroscopy

Raman spectroscopy analyses were carried out on a Witec Alfa 300 spectrometer, with a 532 - nm laser line in backscattering configuration using a microscope with a ×50 objective. The laser power was kept under 0.1 mW to avoid local heat damage to samples. All spectra were acquired with 10 accumulations of 10 seconds of integration time in the region between 100 cm^{-1} and 3,600 cm^{-1}.

Atomic force microscopy

To carry out AFM imaging of the different GO samples, we deposited a diluted solution of each GO on a Si/SiO_2 wafer by drop casting. The drop was carefully rolled over the wafer to uniformly disperse single layers and a few layers of GO. Finally, the excess of solution was blown off with nitrogen (N_2). The samples were dried in ambient conditions for 24 hours. The AFM images were obtained in intermittent contact mode with a JPK Nanowizard 3 using a silicon nitride tip (spring constant of 40 N/m).

Transmission electron microscopy

Dispersed solutions of the different GO materials were used to deposit them on Cu^- holey carbon grids (300 mesh). A probe-corrected FEI Titan 80-300 microscope was used at 80 kV to minimize beam damage effects. Conventional bright

field images and high resolution transmission electron microscopy (HRTEM) images were taken. Electron energy loss spectroscopy (EELS) measurements were done in spectroscopy mode (STEM-EELS) using a GIF 866 camera under the following experimental conditions: α = 58.5 mrad, GIF aperture = 2.5 mrad, dispersion = 0.02 eV/ch with ZLP_{FWHM} resolution of 0.8 eV.

Scanning electron microscopy

The GO solutions were diluted to a concentration of 5 µg/mL using deionized water. One drop of each solution was deposited on a 300-nm SiO_2/Si substrate kept at 50°C on a hot plate and allowed to dry. SEM images were obtained at 15 kV and 50 pA, with secondary electron detection using the Through Lens Detector (TLD-detector) in FEI Helios Nanolab 650.

X-ray photoelectron spectroscopy

XPS analyses were performed in an ultrahigh vacuum medium (pressure of 10^{-9} mbar) using an Mg, Kα (hv = 1,253.6 eV) X-ray source, with power given by emission of 20 mA, at a voltage of 15 kV. For the carbon element, the high-resolution spectra were obtained with analyzer pass energy of 20 eV in steps of 0.05 eV. The binding energies were referred to the carbon 1s level of a neat graphite sample, set as 284.8 eV.

Cell contact to GO

In the literature, many groups have tested the antibacterial activity of GO. Although the early reports were contradictory, a recent study attempted to elucidate the nature of these controversial effects (17). The authors state that the observed antibacterial effect is directly related to the availability of graphene's basal planes, and they further affirm that when GO is exposed to bacteria, its effect is determined by the media in which the 3-hour exposure takes place. If the exposure is carried out in a saline solution, then GO will have an antibacterial effect; when this exposure is carried out in LB broth growth medium, no antibacterial effect was evidenced.

Having these results in mind and to avoid masking antibacterial effects by the medium components, we decided to test the effect our GO-H_2O material for the growth of the gram-negative bacteria *E. coli* (DH5 α), probing 3 different exposure times: 0, 1 and 3 hours in saline solution. Briefly, the experiment consisted of growing *E. coli* at 37°C overnight. Then the culture was changed with fresh medium and allowed to grow again to the exponential phase. *E. coli* at 10^7 colony forming units/mL was resuspended in saline solution (0.9% NaCl) and incubated to a final concentration of 200 µg/mL of GO-H_2O for 1 and 3 hours at 37°C and under agitation. As control, we used samples exposed to Milli-Q grade water. After this step (referred to as exposure), cells along with the materials were harvested by centrifugation, resuspended in 60 mL of fresh medium and incubated at 37°C under agitation (the recovery step) for 500 minutes. For the 0-hour-exposure experiments, the cells were put in contact with the material and immediately allowed to undergo the recovery step (for more details, see "Supplementary material"). After 500 minutes, the optical density at 600 nm (OD_{600}) of the cell cultures was measured, readings were recorded 3 times and all experiments were performed in triplicate.

We tested our materials on mammalian cells by exposing PBMCs to different concentrations of GO-H_2O, GO-PBS and GO-MG, and performed cell viability and apoptosis tests after 24 hours. PBMCs were isolated from the blood of healthy individuals, and a protocol was followed for the separation of PBMCs based on density gradient centrifugation (for further details, see "Supplementary material"). Then the cells were exposed to our materials at concentrations of 2, 20 and 200 µg/mL on multiwell culture plates for 24 hours, including a positive and a negative control. The negative control consisted of only medium and cells, and positive control was 0.3% H_2O_2. We performed trypan blue cell viability tests counting live/dead cells using a hemocytometer.

Results

Sample characterization

We thoroughly studied the physical and chemical properties of our GO materials. AFM, SEM and TEM were used to figure out the morphological characteristics of the different samples, and EELS and XPS to understand their chemistry. Our studies revealed that the GO-H_2O sample contained small fragments of GO with average 2D sizes of 100 nm and thicknesses of 1 or 2 layers (Fig. 1A, D and G; see also "Supplementary material" for more details). The sample GO-PBS was very similar in morphology to GO-H_2O, as can be confirmed in Figure 1B and E. This was not a surprise since both samples were subjected to the same preparation treatment (6 hours in ultrasonic bath); however, the difference between the samples lay in the medium of dispersion (i.e., for GO-PBS, PBS was used). This difference resulted in many PBS residues that accompanied the GO sheets. Figure 1H shows a TEM image of GO-PBS where an impurity can be seen. Furthermore, Figure S2 (available online as supplementary material at www.jab-fm.com) shows an SEM image where the impurities are clearly localized on top of the GO, and our XPS analysis revealed signals from Na, Cl, K and P that evidently came from PBS residues.

Sample GO-MG showed very different characteristics. Figure 1C, f and i reveal that GO-MG contained larger-area GO sheets, averaging several microns, showing similar morphological characteristics to those of exfoliated graphene. Nevertheless, structural damage in the honeycomb structure was detected.

Our XPS analysis of the C binding energies confirmed the presence of sp^2 (C = C) at 283.9 eV and carbon atoms out of regular sp^2 configurations (C-C/C-H) at 284.8 eV as expected for GO (31). Beyond that, other oxygenated carbon functional groups were observed, such as phenol or epoxide (C-OH/C-O-C) between 285.8-286.3 eV, carbonyl groups (C = O) at 287.1 eV, carboxyl groups (COOH) at 288.7 eV and the π-π* shake-up satellite at approximately 291.0 eV typical of aromatic delocalized electrons (32). Figure 2A, B shows XPS spectra of GO-H_2O and GO-MG, respectively. It is clear that although the nature of the bonds present in both samples is the same, their distribution is different. This was expected, as both samples

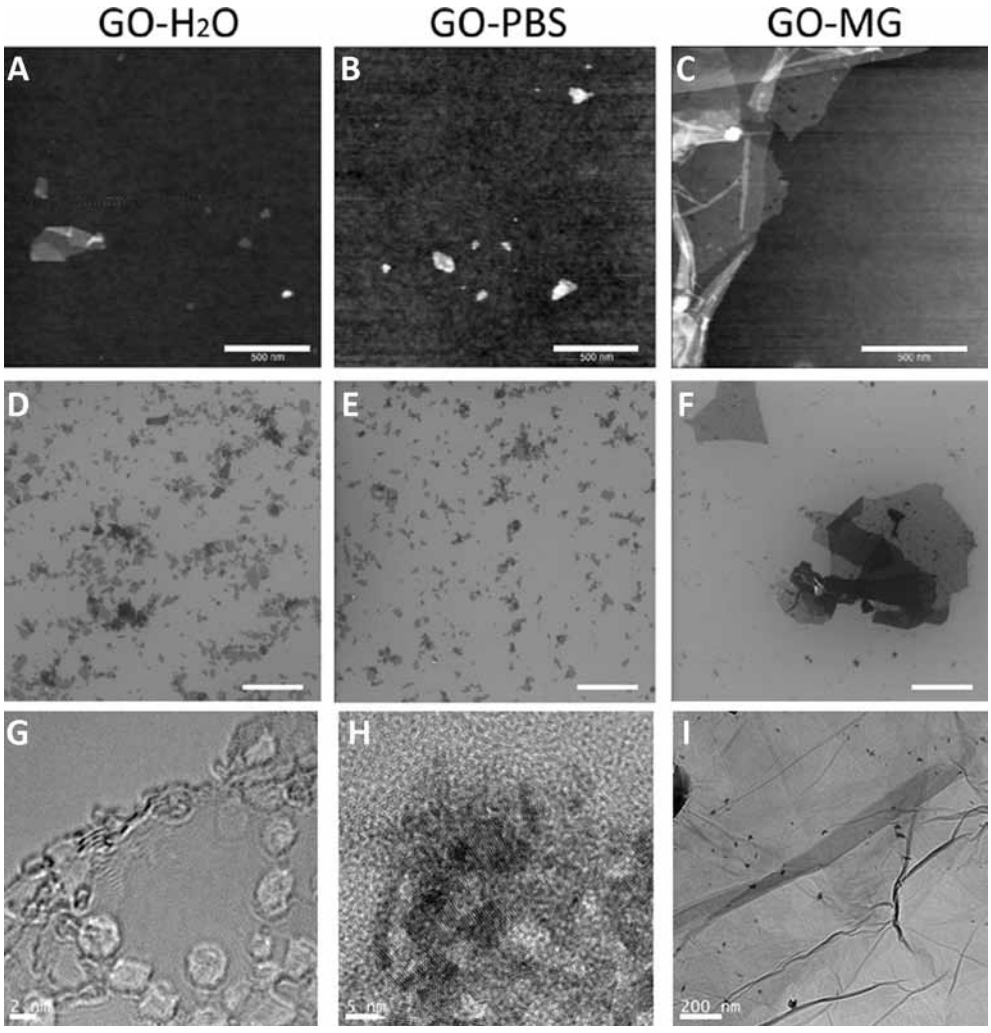

Fig. 1 - Representative atomic force microscopy (AFM) (**A-C**), scanning electron microscopy (SEM) (**D-F**) and transmission electron microscopy (TEM) (**G-I**) micrographs of graphene oxide (GO) samples: (**A, D, G**) GO-H_2O; (**B, E, H**) GO–phosphate-buffered saline (GO-PBS); (**C, F, I**) GO manually ground and dispersed in water (GO-MG). Scale bars represent 500 nm in (**A-C**); 1 µm in (**D-F**); and 2 nm, 5 nm and 200 nm in (**G**), (**H**) and (**I**), respectively.

were derived from GtO and dispersed in water; however, the preparation method led to more sp^2 hybridization in the GO-H_2O sample (18% against 9% in GO-MG; as confirmed by EELS results in Fig. S3, available online as supplementary material at www.jab-fm.com). On the other hand, the oxidized functional groups also showed differences in composition: the most intense component for GO-H_2O were the carbonyl groups (C = O) (25%) (see Suppl Tab. I for information on the EELS analysis, available online as supplementary material at www.jab-fm.com), which were preferentially located on the edges of graphene sheets, while for GO-MG, the most intense component was the third component, C-OH/C-O-C (25%), as shown in Supplemental Table I, typically located on the basal plane of graphene (33).

As mentioned above, the XPS analysis of the GO-PBS sample revealed the presence of elements other than C and O, which were due to the diluent.

Representative Raman spectroscopy results are included in Figure 2C. Bulk measurements of the GO materials revealed the strong presence of the D and G bands, located at ~1,350 cm^{-1} and ~1,590 cm^{-1}, respectively. All spectra shared intense D bands and sharp G bands. We attribute such an intense defect-related band (D band) to the presence of sp^3 hybridization and to the high amount of oxygen bonds which were perforce present on GO. However, the I_D/I_G ratio of the GO-PBS sample was the highest (1.1 compared with 0.97 for both GO-H_2O and GO-MG) probably due to the presence PBS residues, as confirmed by TEM and SEM. From a simple inspection, it is quite obvious that the spectra of the 3 different GO samples are rather similar. For samples GO-H_2O and GO-PBS, this is expected, since the morphology of the samples is comparable (see Fig. 1); however, although sample GO-MG possesses very different characteristics, its Raman spectrum also looks similar. This suggests a high level of defects due to the less regular sp^2 carbon structure, as detected by XPS and EELS. It is possible that the high D band is due to the symmetry breakpoints that arise from in-plane defects (see Fig. 1C), high proportion of sp^3 hybridization, OH-terminated edges and C-O bonds present in the sample.

From our characterization, we can conclude that GO-H_2O and GO-PBS share morphology features (~100 nm, 1-2 layers, amount of defects), while GO-MG presents larger areas but the same average amount of defects. Regarding surface

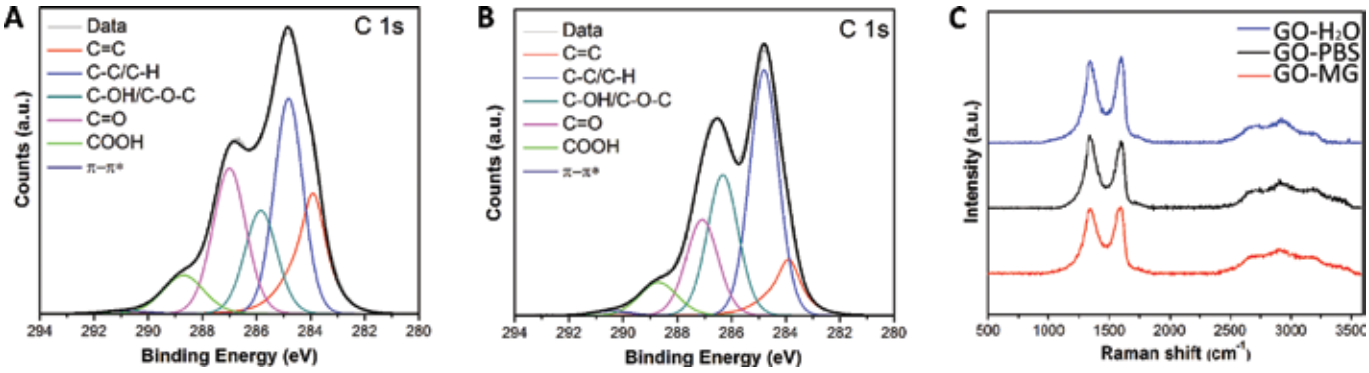

Fig. 2 - (**A, B**) X-ray photoelectron spectroscopy (XPS) spectra of graphene oxide (GO)-H_2O and GO manually ground and dispersed in water (GO-MG), respectively; (**C**) Raman spectra of the GO materials.

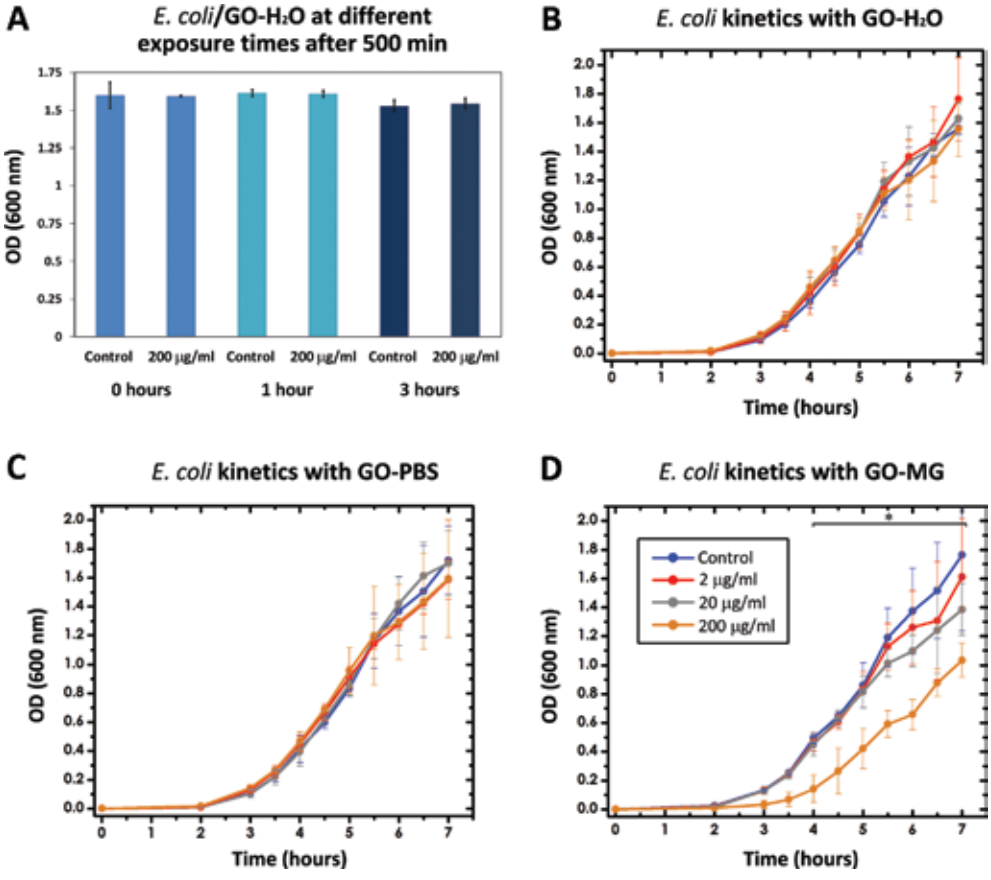

Fig. 3 - (**A**) *E. coli* exposed to graphene oxide (GO)-H_2O at different times (0, 1 and 3 hours) and incubated for 500 minutes in fresh Luria-Bertani medium for a recovery process; (**B-D**) growth kinetics of *E. coli* exposed for 1 hour to different concentrations of GO-H_2O, GO–phosphate-buffered saline (GO-PBS), GO manually ground and dispersed in water (GO-MG), respectively. Inset in (**D**) contains the color codes assigned to the different concentrations used in the study, which apply to graphs (**B-D**). Experiments were performed in triplicate, error bars stand for the standard deviation of the recorded values. OD = optical density; *p<0.05, n = 3.

chemistry, it can be concluded that all samples present a significant amount of sp^3 hybridization and oxygen species.

Biocompatibility tests

Figure 3 shows the growth of *E. coli* in the presence of GO. Our results showed that the presence of GO-H_2O at such a high concentration did not have a negative impact on bacterial cell growth (Fig. 3A). For the 3 exposure times, the OD values of the cultures with GO-H_2O were quite similar to those of controls, suggesting that the amount of living cells did not decrease in contact with GO-H_2O. It is worth mentioning the slight decrease in OD_{600} values for the 3-hour exposure set; both samples (control and GO-H_2O) showed lower values compared with those of the 0-hour and 1-hour exposure sets. We attribute this to a uniform decrease in the amount of living cells after 3 hours of agitation and the decrease of specific growth rate (µ) due to the lack of nutrients in the saline media. To avoid this effect, we chose to perform exposures of 1 hour for our growth kinetic experiments.

To assess the effect of our different GO materials (GO-H_2O, GO-PBS and GO-MG), we performed a 7-hour kinetic

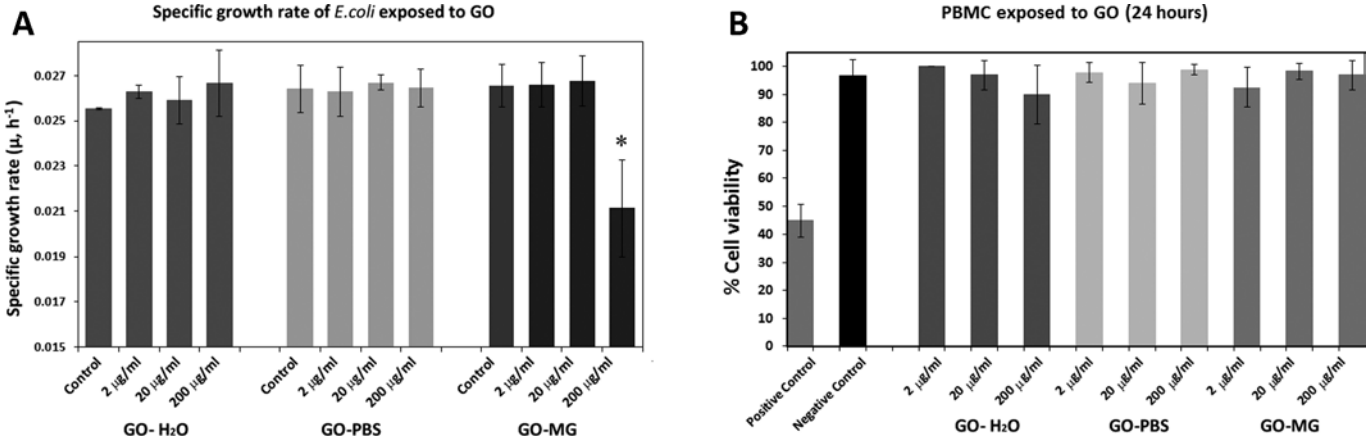

Fig. 4 - (**A**) Specific growth rate of *E. coli* in contact with graphene oxide (GO) materials, calculated from the 7-hour growth kinetic study. *p<0.05, n = 3; (**B**) viability of peripheral blood mononuclear cells exposed to GO materials after 24 hours.

study of the growth of *E. coli*, with an exposure to the materials of 1 hour. We tested 3 different concentrations: 2, 20 and 200 μg/mL for each material. Conditions were similar to those in the above-described experiment (see the section "Cell contact to GO") except that during the recovery step, systematic OD_{600} readings were recorded from the cultures (see more details in "Supplementary material").

Figure 3B, C and D shows the results of our kinetic study of *E. coli* exposed to GO-H_2O, GO-PBS and GO-MG, respectively. From our above-described results. We did not expect to find an antibacterial effect of the GO-H_2O material, and such a conclusion was confirmed by Figure 3B which shows that the 3 concentrations of GO-H_2O tested had no adverse effect on the growth of *E. coli*. Our characterization showed that the morphology of the GO-PBS sample was quite similar to that of GO-H_2O. Thus no antibacterial effect was expected from this sample either. Figure 3C confirms that the presence of GO-PBS at concentrations of 2, 20 and 200 μg/mL did not interfere with the growth of *E. coli*.

Our characterization evidenced the marked differences in morphology that the GO-MG sample presented when compared with GO-H_2O (see Fig. 1). Such differences proved to have a strong impact on the growth of *E. coli* at the highest tested concentration (200 μg/mL). The results of our kinetic study (Fig. 3D) revealed that low doses of GO-MG (2 and 20 μg/mL) do not show any effect on the growth of *E. coli*; however, a higher concentration (200 μg/mL) proved to have an adverse effect on the growth, where μ decreased to a value of 0.021 h^{-1} (±0.002) compared with 0.0265 h^{-1} (±0.0009) for the control (Fig. 4A).

We performed 1- and 2-way ANOVA with Dunnett's post test to compare the different concentrations used against the control. Values of $p < 0.05$ were considered as significant.

We conclude that the sample GO-MG at high concentration shows an antibacterial effect which is the product of the high amount of large-area sheets that wrap around the bacteria, isolating them and disabling their proliferation, in good agreement with the reports of Liu et al (14) and Hui et al (17).

Our study revealed as well that the GO-MG antibacterial effect evidenced here was the product of the interactions with GO during the exposure step, and such an effect was not masked by the presence of LB growth medium during the recovery phase. Furthermore, the absence of this exposure step in saline solution (0-hour exposure) led to a complete suppression of the antibacterial effect of GO-MG (see Suppl Fig. 5, available online as supplementary material at www.jab-fm.com, for results for GO-MG exposed to bacteria), suggesting an adsorption of LB on the surface of the graphene and an inability of the sheets to wrap and isolate *E. coli* – in good agreement with the conclusions drawn by the group of Hui et al (17).

Cytotoxicity to PBMCs

Results for the test of cell viability are shown on Figure 4B, indicating that the presence of GO materials did not have a negative effect on the viability of cells at 24 hours of exposure. The lowest viability identified was for the GO-H_2O sample at the highest concentration tested (200 μg/mL) with a value of 89.95% ± 10.55%. For the rest of the samples, viability was above 90%, proving good hemocompatibility, which is in agreement with previous reports on the subject (22, 27).

Apoptosis tests were conducted on PBMCs exposed to our materials for 24 hours at concentrations of 2 and 20 μg/mL (see details on "Supplementary material").

We evaluated whether our materials induced apoptosis of PBMCs, by flow cytometry using annexin V/propidium iodide markers. Representative dot plots of the apoptosis assay are shown in Figure 5A-E. Interestingly, for all of the materials for both concentrations tested, the percentage of apoptotic cells was very close to that of the negative control (Fig. 5F). In addition, we did not find any increase in necrotic cells when our materials were present, as revealed by the propidium iodide marker, and no early apoptosis was detected, which was revealed when only the annexin marker was used.

It is important to point out that the 24-hour exposure of GO samples to PBMCs described above was done in the presence of RPMI-1640 medium with L-glutamine, 10% fetal bovine serum (FBS) and 1% penicillin-streptomycin (see

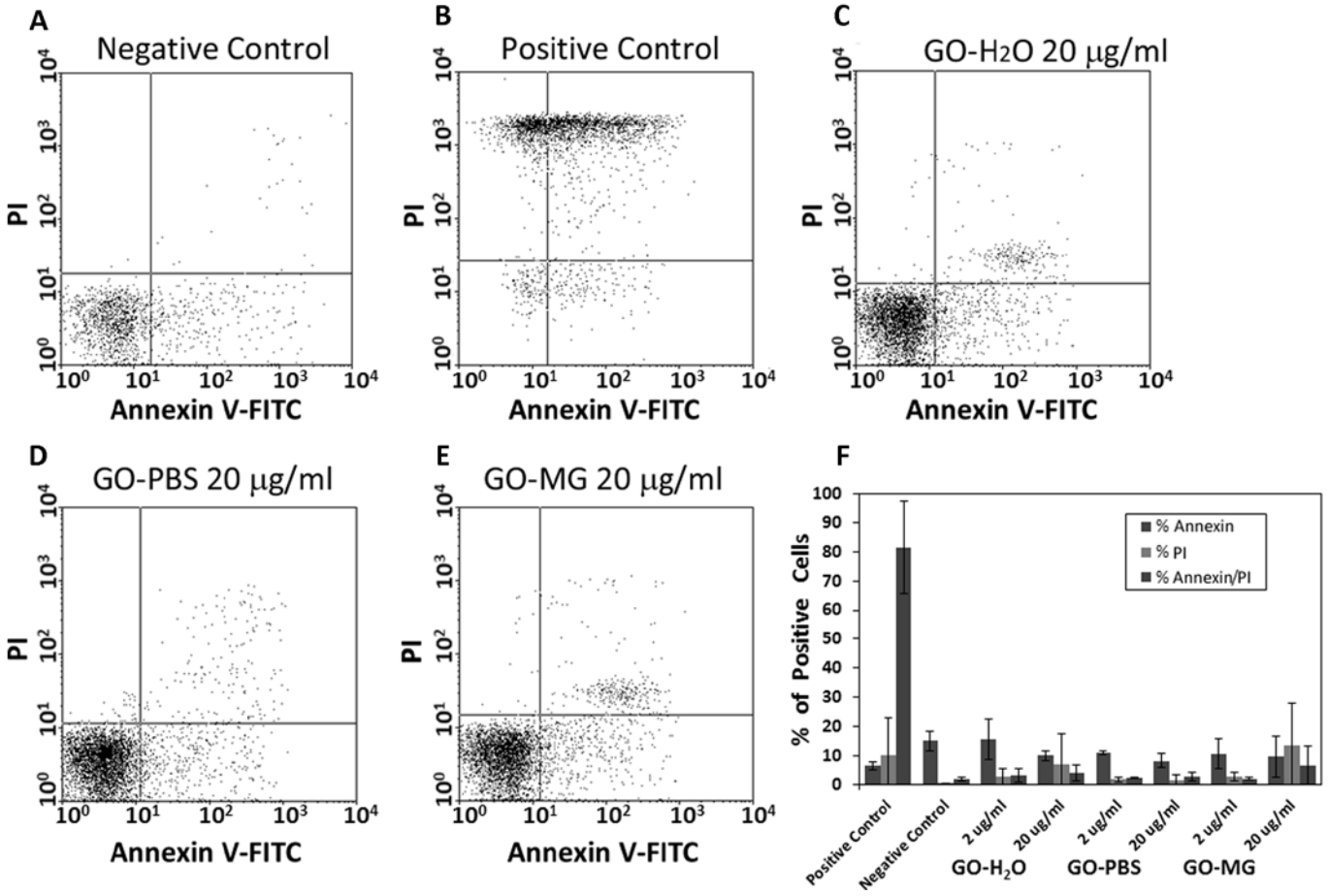

Fig. 5 - Results of the annexin V-FITC and propidium iodide (PI) assay. Representative scatter diagrams of peripheral blood mononuclear cells (PBMCs): (**A**) negative control, (**B**) positive control, (**C-E**) exposed to 20 μg/mL of graphene oxide (GO)-H_2O, GO–phosphate-buffered saline (GO-PBS) and GO manually ground and dispersed in water (GO-MG), respectively; (**F**) summary of the percentage of positive cells for annexin, PI and annexin/PI.

"Supplementary material"). The availability of nutrient molecules from the growth medium opens the possibility of absorption of proteins into the GO basal plane masking thus its toxic effect. To investigate this possibility, new sets of experiments are being designed and performed, in which exposure of GO samples to PBMCs is carried out in the absence of nutrient molecules, as in the case of bacteria.

Discussion

We performed a complete characterization of 3 different GO samples and tested their toxicity to bacteria and PBMCs. GO-H_2O and GO-PBS were obtained by the same preparation method from GtO; a 6-hour sonication treatment produced GO dispersed in water (GO-H_2O) and in PBS (GO-PBS). These samples had 2D dimensions of ~100 nm, consisted of 1-2 staked layers, had sp^3 hybridization and were bonded to oxygen species. GO-MG was derived from GtO by manual grinding and dispersed in water. This preparation led to a material of 1-2 layers with 2D dimensions of several microns possessing many in-plane defects, along with sp^3 hybridization and reactive oxygen species. Our experiments in suspension proved that GO-H_2O and GO-PBS did not show an antibacterial effect to *E. coli*, while the presence of 200 μg/mL of GO-MG decreased its specific growth rate. It is thus evident that not every type of GO will present antibacterial activity; this effect is size-dependent, and small sheets do not interfere with bacteria growth, while large sheets (several microns) tend to inhibit it. We proved as well that the protocol followed for exposure of GO-MG to bacteria was vital for the outcome. While direct exposure of bacteria to all concentrations of GO-MG in LB media did not show an adverse effect; if the first contact was carried out in saline solution for 1-3 hours, then the presence of GO-MG at 200 μg/mL would decrease the specific growth rate of *E. coli*. This observation is in accordance with the results of Hui et al (17) and explains previous contradictory results on the toxicity of GO to bacteria due to protocol discrepancies. Experiments with PBMCs exposed to our GO materials indicated that no adverse effect was observed after 24 hours, in good agreement with previous studies; however, further studies are underway to account for the effect in the absence of nutrient molecules that could be absorbed on the basal planes of GO (22, 27). For

the applications of GO in biology, and in particular, if its antibacterial properties are to be potentiated, it is thus very important to perform a characterization of the material, giving special attention to its dimensions and homogeneity, as well as to the protocol for exposure.

Acknowledgement

We thank B. Archanjo, M. Pojucan, M. Gutiérrez-Hernández and E. H. Ferreira for technical assistance.

Disclosures

Financial support: J.C.-D. is thankful to CONACYT for funding.
Conflict of interest: None of the authors has any financial interest related to this study to disclose.

References

1. Novoselov KS, Geim AK, Morozov SV, et al. Electric field effect in atomically thin carbon films. Science. 2004;306(5696): 666-669.
2. Ferrari AC, Bonaccorso F, Fal'ko V, et al. Science and technology roadmap for graphene, related two-dimensional crystals, and hybrid systems. Nanoscale. 2015;7(11):4598-4810.
3. Chung C, Kim Y-K, Shin D, Ryoo S-R, Hong BH, Min D-H. Biomedical applications of graphene and graphene oxide. Acc Chem Res. 2013;46(10):2211-2224.
4. Sun X, Liu Z, Welsher K, et al. Nano-graphene oxide for cellular imaging and drug delivery. Nano Res. 2008;1(3):203-212.
5. Hu W, Peng C, Luo W, et al. Graphene-based antibacterial paper. ACS Nano. 2010;4(7):4317-4323.
6. Zhang L, Xia J, Zhao Q, Liu L, Zhang Z. Functional graphene oxide as a nanocarrier for controlled loading and targeted delivery of mixed anticancer drugs. Small. 2010;6(4):537-544.
7. Akhavan O, Ghaderi E. Toxicity of graphene and graphene oxide nanowalls against bacteria. ACS Nano. 2010;4(10):5731-5736.
8. Liu S, Zeng TH, Hofmann M, et al. Antibacterial activity of graphite, graphite oxide, graphene oxide, and reduced graphene oxide: membrane and oxidative stress. ACS Nano. 2011;5(9): 6971-6980.
9. Ruiz ON, Fernando KAS, Wang B, et al. Graphene oxide: a nonspecific enhancer of cellular growth. ACS Nano. 2011;5(10): 8100-8107.
10. Das MR, Sarma RK, Saikia R, Kale VS, Shelke MV, Sengupta P. Synthesis of silver nanoparticles in an aqueous suspension of graphene oxide sheets and its antimicrobial activity. Colloids Surf B Biointerfaces. 2011;83(1):16-22.
11. Santos CM, Tria MC, Vergara RA, Ahmed F, Advincula RC, Rodrigues DF. Antimicrobial graphene polymer (PVK-GO) nanocomposite films. Chem Commun (Camb). 2011;47(31):8892-8894.
12. Liao K-H, Lin YS, Macosko CW, Haynes CL. Cytotoxicity of graphene oxide and graphene in human erythrocytes and skin fibroblasts. ACS Appl Mater Interfaces. 2011;3(7):2607-2615.
13. Wojtoniszak M, Chen X, Kalenczuk RJ, et al. Synthesis, dispersion, and cytocompatibility of graphene oxide and reduced graphene oxide. Colloids Surf B Biointerfaces. 2012;89:79-85.
14. Liu S, Hu M, Zeng TH, et al. Lateral dimension-dependent antibacterial activity of graphene oxide sheets. Langmuir. 2012;28(33): 12364-12372.
15. Mangadlao JD, Santos CM, Felipe MJ, de Leon AC, Rodrigues DF, Advincula RC. On the antibacterial mechanism of graphene oxide (GO) Langmuir-Blodgett films. Chem Commun (Camb). 2015;51(14):2886-2889.
16. Akhavan O, Ghaderi E, Esfandiar A. Wrapping bacteria by graphene nanosheets for isolation from environment, reactivation by sonication, and inactivation by near-infrared irradiation. J Phys Chem B. 2011;115(19):6279-6288.
17. Hui L, Piao J-G, Auletta J, et al. Availability of the basal planes of graphene oxide determines whether it is antibacterial. ACS Appl Mater Interfaces. 2014;6(15):13183-13190.
18. Zhang L, Xia J, Zhao Q, Liu L, Zhang Z. Functional graphene oxide as a nanocarrier for controlled loading and targeted delivery of mixed anticancer drugs. Small. 2010;6(4):537-544.
19. Sasidharan A, Panchakarla LS, Chandran P, et al. Differential nano-bio interactions and toxicity effects of pristine versus functionalized graphene. Nanoscale. 2011;3(6):2461-2464.
20. Wang K, Ruan J, Song H, et al. Biocompatibility of graphene oxide. Nanoscale Res Lett. 2011;6:1-8.
21. Chang Y, Yang S-T, Liu JH, et al. In vitro toxicity evaluation of graphene oxide on A549 cells. Toxicol Lett. 2011;200(3): 201-210.
22. Sasidharan A, Panchakarla LS, Sadanandan AR, et al. Hemocompatibility and macrophage response of pristine and functionalized graphene. Small. 2012;8(8):1251-1263.
23. Pinto AM, Gonçalves IC, Magalhães FD. Graphene-based materials biocompatibility: a review. Colloids Surf B Biointerfaces. 2013;111:188-202.
24. Yang K, Li Y, Tan X, Peng R, Liu Z. Behavior and toxicity of graphene and its functionalized derivatives in biological systems. Small. 2013;9(9-10):1492-1503.
25. Seabra AB, Paula AJ, de Lima R, Alves OL, Durán N. Nanotoxicity of graphene and graphene oxide. Chem Res Toxicol. 2014;27(2):159-168.
26. Zhang W, Yan L, Li M, et al. Deciphering the underlying mechanisms of oxidation-state dependent cytotoxicity of graphene oxide on mammalian cells. Toxicol Lett. 2015;237(2): 61-71.
27. Paul W, Sharma CP. Blood compatibility and biomedical applications of graphene. Trends Biomater. Artif. Organs. 2011;25(3): 91-94.
28. Singh SK, Singh MK, Nayak MK, et al. Thrombus inducing property of atomically thin graphene oxide sheets. ACS Nano. 2011;5(6):4987-4996.
29. Jastrzębska AM, Kurtycz P, Olszyna AR. Recent advances in graphene family materials toxicity investigations. J Nanopart Res. 2012;14(12):1320-1341.
30. Guo X, Mei N. Assessment of the toxic potential of graphene family nanomaterials. J Food Drug Anal. 2014;22(1):105-115.
31. Estrade-Szwarckopf H. XPS photoemission in carbonaceuous materials: a "defect" peak beside the asymmetric peak. Carbon. 2004;42(8-9):1713-1721.
32. Rozada R, Paredes JI, Villar-Rodil S, Martínez-Alonso A, Tascón JM. Towards full repair of defects in reduced graphene oxide films by two-step graphitization. Nano Res. 2013;6(3): 216-233.
33. Yang D, Velamakanni A, Bozoklu G, et al. Chemical analysis of graphene oxide films after heat and chemical treatments by X-ray photoelectron and micro-Raman spectroscopy. Carbon. 2009;47(1):145-152.